Hysteresis in the $T=0$ random-field Ising model: Beyond metastable dynamics

Francesc Salvat-Pujol and Eduard Vives
Departament d'Estructura i Constituents de la Matèria, Facultat de Física, Universitat de Barcelona, Martí i Franquès 1, 08028 Barcelona, Catalonia, Spain

Martin-Luc Rosinberg
Laboratoire de Physique Théorique de la Matière Condensée, CNRS-UMR 7600, Université Pierre et Marie Curie, 4 Place Jussieu, 75252 Paris Cedex 05, France

(Received 4 March 2009; published 19 June 2009)

We present a numerical study of the zero-temperature response of the Gaussian random-field Ising model to a slowly varying external field, allowing the system to be trapped in microscopic configurations that are not fully metastable. This modification of the standard single-spin-flip dynamics results in an increase in dissipation (hysteresis) somewhat similar to that observed with a finite driving rate. We then study the distribution of avalanches along the hysteresis loop and perform a finite-size scaling analysis that shows good evidence that the critical exponents associated to the disorder-induced phase transition are not modified.

DOI: 10.1103/PhysRevE.79.061116 PACS number(s): 05.70.Jk, 75.60.Ej, 75.40.Mg, 75.50.Lk

I. INTRODUCTION

The random-field Ising model (RFIM) at zero temperature has been proposed as a prototype for a broad class of disordered systems (random magnets, glasses, plastic and ferroelastic materials, fluids in porous media, etc.) which exhibit an intermittent, avalanchelike, and hysteretic response to a smoothly varying applied force [1]. The RFIM has also been used in several socioeconomics contexts to simulate collective effects induced by imitation and social pressure [2]. A remarkable prediction of the model is the existence of a nonequilibrium critical point (for a certain amount of disorder) which separates two different regimes of avalanches. In the strong-disorder regime, all avalanches are of microscopic size and the saturation hysteresis loop (e.g., magnetization m versus magnetic field H) is macroscopically smooth. At low disorder, a macroscopic avalanche occurs at a certain field, which results in a jump discontinuity in the magnetization. At criticality, avalanche sizes and durations follow power-law distributions.

In the original version of the model [3], spins obey a standard single-spin-flip (Glauber) relaxation dynamics at $T=0$ and align with their local effective field. As the applied field is slowly increased or decreased, a spin may become unstable and then trigger an avalanche that propagates until another metastable state is found. The field is held fixed during the propagation of the avalanche, which corresponds to the so-called "adiabatic" limit. This amounts to assuming that the time for local equilibration (the duration of an avalanche) is much smaller than the rate of change of the driving field. Moreover, by using a deterministic zero-temperature dynamics, one assumes that no thermally activated escape takes place on the observational time scale ("athermal" limit). These two assumptions are reasonable in many physical situations but they are never *fully* satisfied. It is thus interesting to test the robustness of the predicted scenario (in particular the existence of a disorder-induced phase transition and its universality) with respect to a slight violation of these conditions.

In a recent work [4], the influence of partial equilibration processes was mimicked by changing the dynamics and allowing two neighboring spins to flip cooperatively. As expected, this change resulted in a reduction in hysteresis (as the set of two-spin-flip stable states is contained in the set of one-spin-flip stable states) and an enhancement of large-scale collective effects [5]. But, remarkably, the critical behavior (characterized by various exponents and finite-size scaling functions) remained identical. In the present work, we want to go in the opposite direction by *enlarging* the set of visited microscopic states to increase hysteresis and drive the system further from equilibrium. This is done by allowing a small fraction of the spins to point in the opposite direction to their local field. However, in order to keep things as simple as possible (and, in particular, to keep the simplifying separation of motion between adiabatic driving and avalanche propagation), we will still use a single-spin-flip dynamics and start an avalanche when some threshold in energy is reached. As a consequence, the saturation loop will not be an "extremal" path in the field-magnetization plane [6,7] and the property of return-point memory [3] will be violated. The main question that we want to address is: will this change the universal properties of the critical behavior? Note that this modification of the dynamical rule may be viewed as a crude way of simulating the effect of a finite driving rate which does not give enough time to the system to relax, even locally [8–12]. But this is of course a caricature of what happens in the real world and we therefore do not pretend to propose here a theory of dynamic hysteresis, a topic that has been (and still is) intensively investigated in the literature [13]. In a socioeconomic context, one could also interpret this model as simulating an effect of "inertia" that prevents the individual agents to make their decision (e.g., buy or sell) when the incentive reaches the threshold value.

The paper is organized as follows. In Sec. II, we describe the model and the dynamics, and discuss some of its properties. In Sec. III, we study the hysteresis loops, in particular the change in coercivity. Avalanche distributions are analyzed in Sec. IV and the critical behavior in Sec. V. Summary and conclusion are given in Sec. VI.

II. MODEL AND DYNAMICS

We consider the RFIM on a three-dimensional (3D) cubic lattice of linear size L with periodic boundary conditions. On each site i there is a spin variable $S_i = \pm 1$. The energy of the system of $N=L^3$ spins is described by the Hamiltonian

$$\mathcal{H} = -J\sum_{\langle ij\rangle} S_i S_j - \sum_i h_i S_i - H\sum_i S_i, \tag{1}$$

where $J>0$ is a ferromagnetic exchange interaction constant and the first sum runs over nearest-neighbor pairs. Without loss of generality, we will take $J=1$. The set of random fields $\{h_i\}$ is drawn independently from a Gaussian probability distribution with zero mean and variance σ^2, and H is a uniform external magnetic field which couples to the overall magnetization $M=\Sigma_i S_i (m=M/N)$.

The energy change associated to the reversal of spin i then reads

$$\Delta\mathcal{H}_i \equiv \Delta\mathcal{H}(S_i \to -S_i) = 2S_i F_i, \tag{2}$$

where

$$F_i = \sum_{j/i} S_j + h_i + H \tag{3}$$

is the local effective field acting on spin i, and j is a nearest neighbor of i.

At $T=0$ the standard single-spin-flip dynamics consists in flipping a spin if this lowers its energy. A configuration is thus single-spin-flip stable if every spin is aligned with its local field, i.e.,

$$S_i = \mathrm{sgn}(F_i) \quad \forall\, i. \tag{4}$$

Each of these metastable states has a certain range of stability $H_{min} \le H \le H_{max}$.

As the field H is slowly changed, a spin flips (either upward or downward) when its local field changes sign, which may induce a whole avalanche of other spin flips. In the adiabatic limit H is held constant during the propagation of the avalanche. The avalanche stops when a new metastable state is reached. A nice feature of this dynamics is that it is "Abelian:" because of the so-called "no-passing" rule [3], the metastable state reached at the end of an avalanche is independent of the order in which unstable spins have been reversed. In consequence, these spins can be flipped either sequentially or in parallel (this latter choice having the advantage that one can define the duration of an avalanche).

We now modify this dynamical rule by allowing a certain number of spins to be unstable [Eq. (4) is then violated]. This can be done in various ways, for instance, by imposing that the fraction of unstable spins cannot exceed a certain value. This, however, would prevent the system to reach saturation. We therefore prefer to compute the extra amount of energy associated to the unstable spins and impose that an avalanche starts when this contribution exceeds some fixed threshold ϵ. Specifically, the system may visit spin configurations that we call "ϵ stable" and that satisfy

$$\sum_{S_i \text{unstable}} \Delta\mathcal{H}_i \ge -N\epsilon, \tag{5}$$

where the sum runs over all unstable spins, i.e., spins for which $\Delta\mathcal{H}_i < 0$ (note that ϵ is an intensive quantity). There are now two conditions for an avalanche to start: (i) there must be unstable spins and (ii) the sum of the extra contributions to the energy due to the unstable spins must exceed the threshold (in absolute value). When increasing (respectively, decreasing) the field, only negative (respectively, positive) spins contribute to this energy. One of course recovers the usual dynamics for $\epsilon=0$.

It is quite obvious that this modification of the dynamics spoils the no-passing rule and the Abelian property. Therefore, since several spins may be unstable when the energy threshold is reached, one needs to specify the order in which these spins are flipped. The natural choice that we adopt is to flip the most unstable spin first, which is the one that corresponds to the most negative $\Delta\mathcal{H}_i$. We then update the local fields while keeping H constant, search again for the most unstable spin, flip it, etc., until Eq. (5) is satisfied [14]. This "greedy" algorithm essentially amounts to performing a steepest descent path in energy, which defines a deterministic sequence of unstable states inside an avalanche (defined as usual as the collection of spins which flip at the same field). It is then not difficult to see that the order in which the spins are flipped along the hysteresis loop *does not* depend on ϵ, so that the sequence of visited states is invariant. Changing ϵ only changes the values of the external field at which the states are reached or left. More generally, in any monotonous field history from a state with magnetization M to a state with magnetization M', the sequence of visited spin configurations does not depend on ϵ, but the corresponding fields may differ. As a result, avalanches may split or merge when changing ϵ so that their number and size also change. This is illustrated in Fig. 1 where we compare the hysteresis loops obtained for $\epsilon=0$ and $\epsilon=0.03$ in a small size system. One can see in Figs. 1(b) and 1(c) that the spin configurations at a given magnetization M are identical although the hysteretic trajectories are different. Figure 1(b) also shows that a state which is not single-spin-flip stable for $\epsilon=0$ (as it is located in the middle of an avalanche) is ϵ stable for $\epsilon=0.03$. In Fig. 1(c), the opposite situation is observed.

The fact that the modified dynamics does not satisfy the no-passing rule has two consequences. First, there can exist ϵ states outside the hysteresis loop [7]. Second, the property of return-point memory (RPM) is not satisfied as shown in Fig. 2. However, the violation of RPM is small for the values of ϵ considered in this work and it seems that this property is better and better verified as the system size increases. One can also see in Fig. 2 that the first-order reversal curves have a linear portion: when reversing the field (for instance from H_0 to H_1), the negative spins that were unstable at H_0 become stable again before any positive spin becomes unstable and Eq. (5) is only violated when $H < H_2$.

As a final remark in this section, we compare the proposed dynamics with the algorithms that have been used previously to study the $T=0$ RFIM with a finite driving rate [8,10–12]. The most common strategy consists in increasing

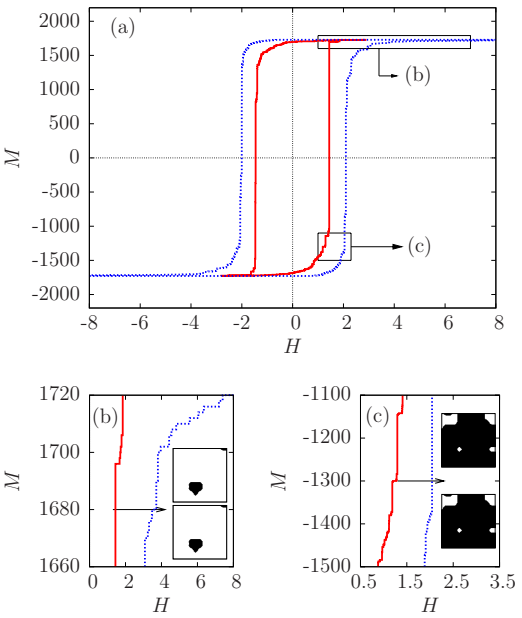

FIG. 1. (Color online) Comparison of the hysteresis loops obtained with $\epsilon=0$ (solid line) and $\epsilon=0.03$ (dashed line) in a system of linear size $L=12$. In (b) and (c) the upper and lower parts of the ascending branches are blown up showing that some avalanches merge or split when ϵ is changed. For a given overall magnetization M, the reached configurations are identical (as illustrated by two-dimensional slices of the system where negative spins are drawn in black), but the corresponding fields are different.

the field in finite steps ΔH, thus merging all the avalanches occurring within that field window into a larger avalanche [8,11,12]. The resulting magnetization loops then share a series of common points with those obtained with the adiabatic driving. On the other hand, in our case avalanches not only merge but also split and the resulting loops differ everywhere from the adiabatic ($\epsilon=0$) loops. A second strategy [10,11] consists in performing an exact simulation of the continuous $M(t)$ signal by using a finite driving rate and defining a time interval associated to the shell of spins that relax in parallel. But one then needs to fix a threshold to define the avalanches

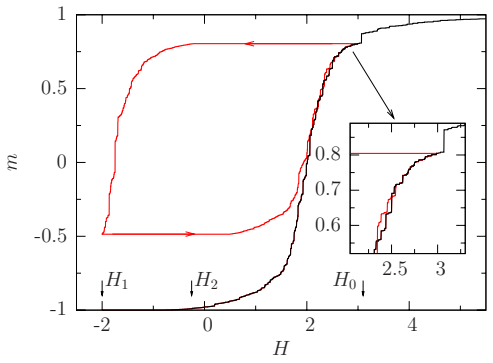

FIG. 2. (Color online) Test of the return-point memory property in a system of linear size $L=12$ for $\sigma=3.5$ and $\epsilon=0.05$. The field is increased up to H_0, decreased from H_0 to H_1, and then increased again up to saturation. The return trajectory crosses the ascending branch of the saturation hysteresis loop several times indicating that ϵ states exist outside the loop and that the RPM property is violated.

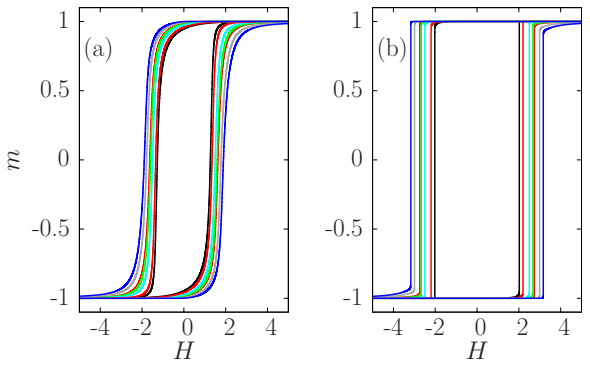

FIG. 3. (Color online) Average hysteresis loop for $\sigma=2.8$ (a) and $\sigma=1.5$ (b). The curves correspond, respectively, to $\epsilon=0$ (inner loop), 0.0005, 0.004, 0.008, 0.01, 0.02, and 0.03 (outer loop). Data result from an average over 5000 disorder realizations in a system of size $L=24$.

and this has a strong influence on their size [15]. This problem does not occur in the modified dynamics that we used here since there is still a complete time-scale separation between the field driving and the propagation of the avalanches.

III. HYSTERESIS LOOPS

We first consider the influence of ϵ on the shape of the hysteresis loops for different values of the disorder strength σ. Figure 3 shows the results obtained by averaging over different disorder realizations for $\sigma=2.8$ and $\sigma=1.5$. As expected, the main effect of ϵ is to bring the system further away from equilibrium and to increase hysteresis. For $\sigma=3$, for instance, the loop area, which represents the energy loss, increases by $\sim 70\%$ when increasing ϵ from 0 to 0.03. This is already an important variation and in the following we shall restrict our study to the range $0 \leq \epsilon \leq 0.03$.

Figure 3 also shows that there are still two different regimes when $\epsilon \neq 0$ and that the shape of the loops changes from smooth to rectangular as σ decreases. In particular, at low disorder, there is a single avalanche that spans the whole system at a certain value of the external field (note that the spanning avalanche in a finite system occurs with no collective precursor for $\epsilon > 0.03$, which may change its nature. This is also a reason to restrict our study to smaller values of ϵ).

To further quantify the influence of ϵ on the hysteresis, we show in Fig. 4 the variation in the coercive field H_{coer} for different values of the disorder. We find that the data are quite accurately fitted by the equation

$$H_{coer}(\epsilon) = H_{coer}(0) + C\epsilon^{\beta}, \tag{6}$$

with $\beta \approx 0.5$ in the large-disorder regime and $\beta \approx 0.45$ at low disorder [16]. The same dependence is found for the variations in the loop area with ϵ. So far, we have no convincing theoretical explanation for this behavior. On the other hand, it appears that the same exponent $\beta \approx 0.45$ in the low-disorder regime has been observed in a simulation study of the RFIM under a linear driving rate [9] (in that study, how-

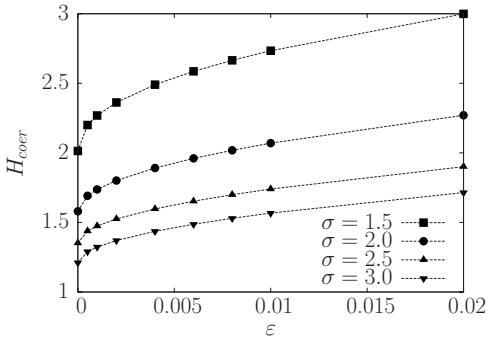

FIG. 4. Average coercive field as a function of ϵ for different values of σ. The data result from an average over 500 disorder realizations in a system of size $L=24$ and are fitted according to Eq. (6).

ever, there is no clear scaling at large disorder). In two dimensions [12], when varying the field in small steps as in Ref. [11], simulations show a crossover from a square-root to a linear dependence of H_{coer} with the rate as the disorder is increased, in agreement with the behavior observed in ferromagnetic thin films.

IV. AVALANCHE SIZE DISTRIBUTION

The RFIM with the standard ($\epsilon=0$) dynamics displays a power-law distribution of avalanche sizes at a critical disorder $\sigma=\sigma_c$ [3]. Depending on the method used to extrapolate the numerical results to the thermodynamic limit, the value of σ_c varies from 2.16 [17] to 2.21 [18,19]. In this section we study the behavior of the avalanche size distribution for $\epsilon>0$.

Figure 5 shows the avalanche size distribution $D(s;\sigma,\epsilon,L)$ obtained in a system of size $L=30$ for $\epsilon=0.008$ and various disorders σ when sweeping through a half loop. The same behavior as for $\epsilon=0$ is observed: for large σ the distribution is exponentially damped whereas for

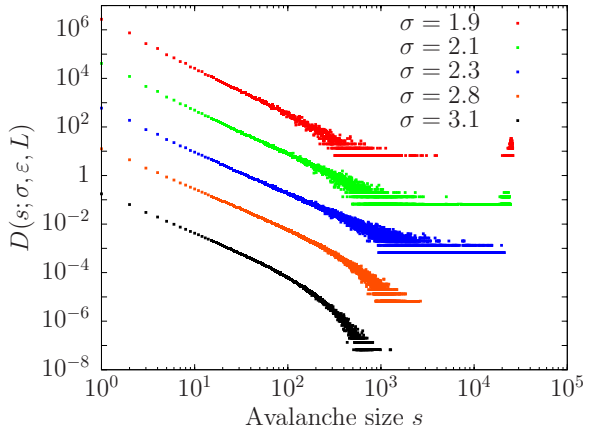

FIG. 5. (Color online) Avalanche size distributions in a system of size $L=30$ for $\epsilon=0.008$ and different values of σ. The curves are sorted from top to bottom in the order indicated in the legend. The statistics has been performed over 1500 disorder realizations. Data for $\sigma\neq 2.3$ have been shifted vertically.

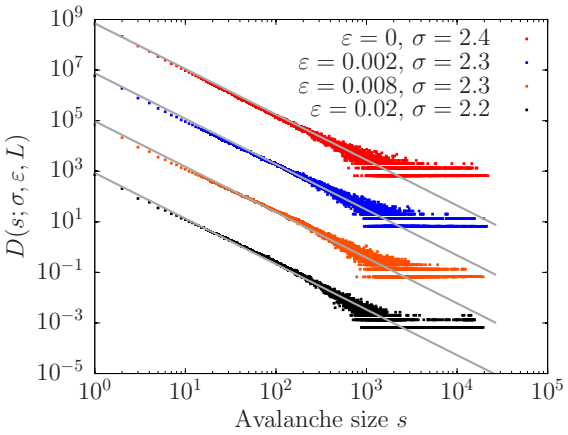

FIG. 6. (Color online) Avalanche size distributions in a system of size $L=30$ for different values of ϵ. The curves are sorted from top to bottom in the order indicated in the legend. In each case, the disorder σ is the one for which the distribution is closest to a power law. The slope of the dashed lines that describe the power-law region is -1.8. The statistics has been performed over 1500 disorder realizations. Data for $\epsilon\neq 0.02$ have been shifted vertically.

small σ there is a peak at large sizes due to avalanches with characteristic size $\sim L^3$. These spanning avalanches are responsible for the macroscopic discontinuity in the hysteresis loop. Between these two regimes, there is a value of σ for which the distribution is very well approximated by a power law up to the trivial cutoff size $s_{max}\sim L^3$ (and apart from some corrections at very small s). This "critical" value of σ changes with ϵ but the slope of the power-law region appears to be invariant as shown in Fig. 6. We view this result as a first indication that there exists a critical disorder $\sigma_c(\epsilon)$ in the thermodynamic limit and that the power-law exponent $\tau+\sigma\beta\delta$ that characterizes the avalanche size distribution at criticality [3] does not change with ϵ (note that the numerical value obtained in a finite system may differ from the actual value ~ 2 in the thermodynamic limit, as estimated in Ref. [3]). In the next section we present a finite-size scaling analysis that will corroborate this statement.

Note that this result contrasts with the one that has been obtained in previous studies using a finite driving rate [10,11]. Indeed, when the only effect of the finite driving rate is to merge small avalanches into larger ones, the power-law exponent decreases. It is in fact unclear if such a decrease is due to the actual out-of-equilibrium behavior or is induced by the approximate treatment of the avalanche merging phenomenon and/or by the definition of the threshold that allows to discriminate the avalanches.

V. CRITICAL PROPERTIES

The analysis of the spanning avalanches has proven to be a successful way to determine the values of several critical exponents in the RFIM with the standard metastable dynamics [18,19]. Indeed, the statistics of spanning avalanches in finite systems contains information about the percolating fractal avalanches in the thermodynamic limit which are the signature of criticality. In this section we use a finite-size

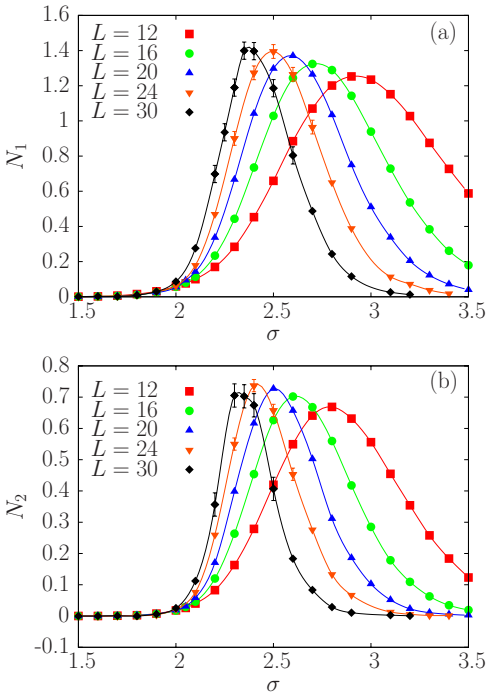

FIG. 7. (Color online) Average number of (a) 1D- and (b) 2D-spanning avalanches as a function of σ for $\epsilon=0.008$ and different system sizes. Typical error bars for the largest sizes are shown.

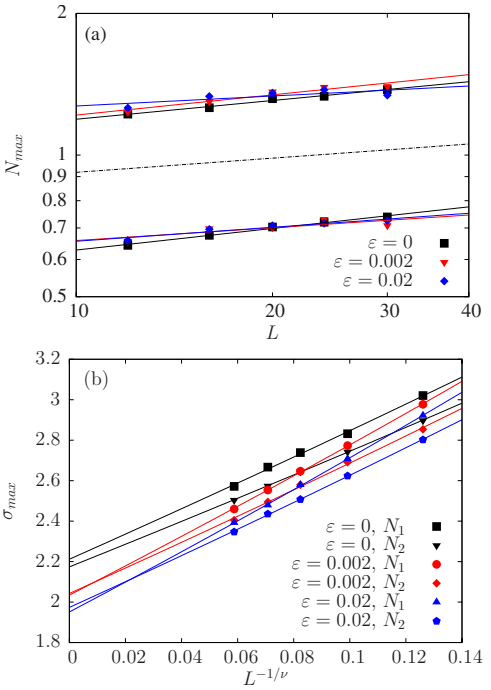

FIG. 8. (Color online) Height and position of the peak in $N_1(\sigma,\epsilon,L)$ and $N_2(\sigma,\epsilon,L)$ for different values of ϵ and different system sizes. In (a), the height is plotted vs L in a log-log plot and in (b) the position is plotted vs $L^{-1/\nu}$ with $\nu=1.2$. The data are fitted according to Eq. (7) with $A=-0.1$. The dotted line in (a) has a slope 0.1 and is included as a reference.

scaling method to study the effect of ϵ on the critical behavior of the model.

With the modified dynamics ($\epsilon>0$) an avalanche still involves a connected set of spins and the spanning avalanches can be defined as usual: avalanches that span the whole system in one, two, or three spatial dimensions are referred to as one-dimensional (1D)-, two-dimensional (2D)-, and 3D-spanning avalanches, respectively. We focus our analysis on the average number of 1D- and 2D-spanning avalanches occurring along the lower branch of the hysteresis loop, which we call $N_1(\sigma,\epsilon,L)$ and $N_2(\sigma,\epsilon,L)$, respectively. We discard from our analysis the 3D-spanning avalanches, which contain information not only about the critical percolating avalanches, but also about the compact infinite avalanche that gives rise to the first-order discontinuity in the low-disorder regime [18].

Figure 7 illustrates the behavior of $N_1(\sigma,\epsilon,L)$ and $N_2(\sigma,\epsilon,L)$ as a function of σ for $\epsilon=0.008$ and different system sizes (the data correspond to averages over typically 10^3-10^4 disorder realizations). One can see that both functions exhibit a peak whose height increases with L. Moreover the peak position shifts and its width reduces. These features are clear signatures of the existence of an infinite number of percolating avalanches at a certain critical disorder $\sigma_c(\epsilon)$ in the thermodynamic limit. $N_1(\sigma,\epsilon,L)$ and $N_2(\sigma,\epsilon,L)$ are thus expected to have the scaling form [17,18]

$$N_1(\sigma,\epsilon,L)=L^{\theta}\hat{N}_1(uL^{1/\nu},\epsilon), \tag{7}$$

$$N_2(\sigma,\epsilon,L)=L^{\theta}\hat{N}_2(uL^{1/\nu},\epsilon), \tag{8}$$

where $\hat{N}_1$ and $\hat{N}_2$ are finite-size scaling functions, $u(\sigma)$ is some analytical function of the distance to the critical disorder, and θ and ν are critical exponents that characterize the divergence of the number of spanning avalanches and of the correlation length, respectively. Although the function $u(\sigma)$ can be approximated to first order as $[\sigma-\sigma_c(\epsilon)]/\sigma_c(\epsilon)$, previous studies [18] suggest that higher-order terms are necessary to produce good scaling collapses. Therefore, as in Ref. [18], we shall use

$$u=\frac{\sigma-\sigma_c(\epsilon)}{\sigma_c(\epsilon)}+A(\epsilon)\left(\frac{\sigma-\sigma_c(\epsilon)}{\sigma_c(\epsilon)}\right)^2, \tag{9}$$

where $A(\epsilon)$ is a nonuniversal parameter that may depend on ϵ. For $\epsilon=0$, the best choice was found to be $A=-0.2$. This value did not change when replacing the one-spin-flip by the two-spin-flip dynamics [4].

Equations (7) and (8) may be first tested by plotting the height of the peaks in $N_1(\sigma,\epsilon,L)$ and $N_2(\sigma,\epsilon,L)$ as a function of L in a log-log scale. As shown in Fig. 8(a), the behavior is then linear and the slope is compatible with the value $\theta=0.1$ obtained for $\epsilon=0$ [18].

A second test consists in plotting the position σ_{max} of the peaks as a function of $L^{-1/\nu}$, as shown in Fig. 8(b). From Eqs. (7) and (8), this position should be determined by the condition $uL^{-1/\nu}=$constant, i.e.,

$$KL^{1/\nu}=\frac{\sigma_{max}(\epsilon)-\sigma_c(\epsilon)}{\sigma_c(\epsilon)}+A\left(\frac{\sigma_{max}(\epsilon)-\sigma_c(\epsilon)}{\sigma_c(\epsilon)}\right)^2. \tag{10}$$

For $A=0$ this equation predicts a linear behavior of σ_{max} as a function of $L^{-1/\nu}$. As can be seen in Fig. 8(b), the actual

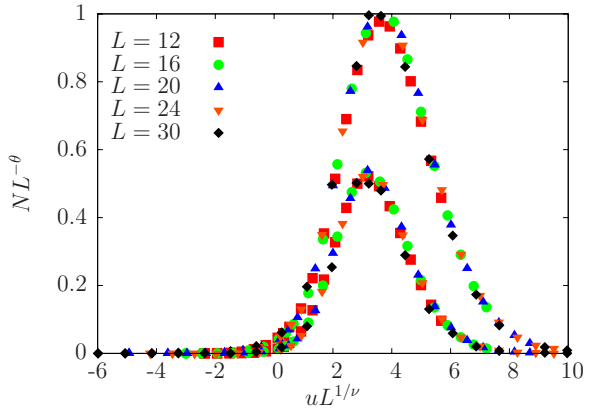

FIG. 9. (Color online) Scaling plot of the number of 1D- and 2D-spanning avalanches for $\epsilon=0.008$ and different system sizes. The upper (resp. lower) curve corresponds to the 1D-(resp. 2D-) spanning avalanches using $\sigma_c=1.97$, $A=-0.1$, $\theta=0.1$, and $\nu=1.2$.

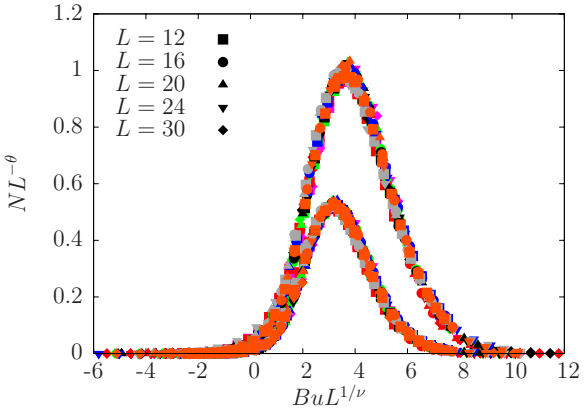

FIG. 10. (Color online) Scaling plot of the number of 1D-(upper curves) and 2D-(lower curves) spanning avalanches according to Eqs. (11) and (12) for different system sizes L (indicated by different symbols) and for $\varepsilon=0.001, 0.002, 0.006, 0.008, 0.01, 0.02, 0.03$ (not indicated).

behavior is indeed almost linear when using the value $\nu=1.2$ obtained for $\epsilon=0$ [18] and the data for the 1D- and 2D-spanning avalanches reasonably extrapolate toward the same value in the thermodynamic limit $L\to\infty$. This method, however, cannot be used to extract accurate values of A or $\sigma_c(\epsilon)$ and the fits shown in Fig. 8(b) are based on the results of the finite-size scaling analysis that we now discuss.

Indeed, the best way to estimate all universal and nonuniversal parameters is to search for a good collapse of the curves $N_1(\sigma,\epsilon,L)$ and $N_2(\sigma,\epsilon,L)$ corresponding to different sizes L. This is done by plotting $N_1(\sigma,\epsilon,L)L^{-\theta}$ as a function of the scaling variable $uL^{1/\nu}$. As an example, we show in Fig. 9 the best collapse obtained for $\epsilon=0.008$ using the values $\sigma_c=1.97$, $A=-0.1$, $\theta=0.1$, and $\nu=1.2$. This procedure can be done independently for each set of data corresponding to different ϵ. Table I shows the parameters that produce the best collapses of the curves for $0.0005\leq\epsilon\leq0.03$ [20] For comparison we also include the results obtained for $\epsilon=0$ [18]. In all cases, the values $\nu=1.2$, $\theta=0.1$, and $A=-0.1$ are the best estimates. The only parameter showing a clear dependence with ϵ is σ_c. Notice that A, which in principle is a nonuniversal parameter, takes the same value -0.1 for all $\epsilon>0$. For $\epsilon=0$ the value $A=-0.2$ produced a better collapse [18] but the difference is not very significant since the collapse in Fig. 9 is still rather good when using this value (alternatively, one can also use $A=-0.1$ for $\epsilon=0$).

TABLE I. Universal and nonuniversal parameters that yield the best finite-size scaling collapses for different values of ϵ.

ϵ	ν	θ	σ_c	A	B
0	1.2	0.1	2.21	−0.2	1.26
0.0005	1.2	0.1	2.035	−0.1	1.05
0.001	1.2	0.1	2.02	−0.1	1.04
0.002	1.2	0.1	2.02	−0.1	1.02
0.006	1.2	0.1	1.98	−0.1	1.01
0.008	1.2	0.1	1.97	−0.1	1.00
0.01	1.2	0.1	1.97	−0.1	1.01
0.02	1.2	0.1	1.96	−0.1	1.02
0.03	1.2	0.1	1.97	−0.1	1.02

The most important feature in Table I is that the two critical exponents ν and θ do not change with ϵ and are the same as for $\epsilon=0$. This suggests that the critical behavior is described by the same universality class. We then try to collapse all the data for different ϵ and L on the same plot by introducing a nonuniversal scale factor B that is ϵ dependent, i.e., by assuming that

$$N_1(\sigma,\epsilon,L)=L^{\theta}\hat{N}_1[B(\epsilon)uL^{1/\nu}], \tag{11}$$

$$N_2(\sigma,\epsilon,L)=L^{\theta}\hat{N}_2[B(\epsilon)uL^{1/\nu}]. \tag{12}$$

As can be seen in Fig. 10, a very good collapse of the whole set of curves in the range $0.0005\leq\epsilon\leq0.03$ is obtained with the values of B indicated in Table I (this scale factor is arbitrarily set equal to 1 for $\epsilon=0.008$).

A cross-check of the consistency of the scaling collapses can be done by fitting the data in Fig. 8(b) using Eq. (10) with $\nu=1.2$ and $A=-0.1$. The extrapolated values of σ_c for $L\to\infty$ are fully compatible with those reported in Table I.

Our data are thus consistent with the fact that the disorder-induced critical point found for $\epsilon=0$ transforms into a critical line when $\epsilon>0$ and the system is allowed to visit weakly unstable states. The whole critical line appears to be described by the same exponents and by the same scaling function for $\epsilon>0$. On the other hand, it seems that the scaling function differs from the one corresponding to $\epsilon=0$, as shown in Fig. 11 on a linear-log scale (in the figure, B is chosen so as to produce the best collapse on the right-hand side of the peak; for $\epsilon=0$, this yields $B=1.35$ and $A=-0.1$ but the picture essentially does not change with $A=-0.2$).

The fact that the exponents ν and θ are the same but the scaling functions are different for $\epsilon=0$ and $\epsilon>0$ may be surprising at first sight. On the one hand, this may simply indicate that higher-order terms in the scaling variable u are needed [let us recall again that the simplest choice $u=(\sigma-\sigma_c)/\sigma_c$ does not produce good scaling collapses and that it

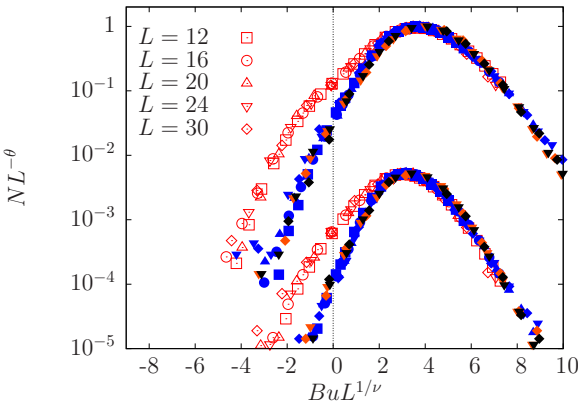

FIG. 11. (Color online) Comparison of the scaling functions $\hat{N}_1$ (above) and $\hat{N}_2$ (below) for $\epsilon=0$ (empty symbols) and $\epsilon>0$ (filled symbols) on a linear-log scale. Different symbols indicate the system size. $\hat{N}_2$ has been shifted two decades downward for clarity.

was proposed already in Ref. [3] to use $u=(\sigma-\sigma_c)/\sigma$, which amounts to keeping an infinite number of terms in an expansion in powers of $(\sigma-\sigma_c)/\sigma_c$]. It is clear that simulations with much larger system sizes would be required to fully settle this issue [21]. On the other hand, there may be indeed an essential physical difference in the properties of the percolating clusters at the critical point. This may not change the fractal dimension (as this would be reflected in a change of the critical exponents) but only the way the finite size affects the number and size of these clusters. It can be seen for instance in Fig. 11 that the number of 1D- and 2D-spanning avalanches diverges like $\sim L^{0.1}$ at the critical point $u=0$ but that the prefactor of this divergence dramatically decreases as soon as ϵ becomes slightly positive. Finite-size scaling functions are known to depend sensitively on boundary conditions and, in the present case, they may account for the fact that the percolating clusters are growing in a different environment when $\epsilon>0$. Recall that we are dealing here with a nonequilibrium phenomenon and that, in the original model [17], a finite fraction of the system has already transformed when the critical point is reached. This is reflected in the value of the critical magnetization M_c. It is not easy to estimate the actual value of this quantity in the thermodynamic limit, but preliminary calculations suggest that M_c significantly decreases when $\epsilon>0$ (even for $\epsilon=0.0005$), showing that the fraction of spins that flip when driving the system from $H=-\infty$ to the critical field $H_c(\epsilon)$ becomes very small.

VI. SUMMARY AND CONCLUSION

We have studied the zero-temperature random-field Ising model, with a Gaussian distribution of the random fields, using a modified single-spin-flip dynamics that allows the system to be trapped in weakly unstable states when driven quasistatically by an external field. The dynamics, however, does not modify the sequence of states that are visited during a monotonous field history and preserves the intermittent avalanchelike character of the response to the driving field. The violation of the standard local stability condition is controlled by a single parameter ϵ whose effect is somewhat similar to that of a finite-driving rate, moving the system away from equilibrium and resulting in a similar increase in the width of the saturation hysteresis loop, as measured by the coercive field. Avalanches are modified but two distinct regimes of avalanches and two different loop shapes as a function of disorder are still present. As in the original model [3], the transition between the two regimes corresponds to a critical point where avalanches of all sizes are observed. The critical exponents that have been extracted from a finite-size scaling analysis of the number of the spanning avalanches appear to be independent of ϵ, suggesting that the condition of strict metastability (as well as the no-passing rule) may be irrelevant for the critical behavior. In our opinion, this significantly enlarges the domain of validity of the original model.

ACKNOWLEDGMENTS

This work received financial support from CICyT (Spain) under Project No. MAT2007-61200 and CIRIT (Catalonia) under Project No. 2005SGR00969. F.S.-P. acknowledges a post-graduate studies grant from the Fundació "la Caixa".

[1] See J. P. Sethna, K. A. Dahmen, and O. Perković, in *The Science of Hysteresis*, edited by G. Bertotti and I. Mayergoyz (Academic Press, Amsterdam, 2006) (and references therein).
[2] See, e.g., Q. Michard and J. P. Bouchaud, Eur. Phys. J. B **47**, 151 (2005) for a recent and concrete application of the model to several social phenomena.
[3] J. P. Sethna, K. A. Dahmen, S. Kartha, J. A. Krumhansl, B. W. Roberts, and J. D. Shore, Phys. Rev. Lett. **70**, 3347 (1993).
[4] E. Vives, M. L. Rosinberg, and G. Tarjus, Phys. Rev. B **71**, 134424 (2005).
[5] This is illustrated by exact calculations performed on the Bethe lattice, X. Illa, M. L. Rosinberg, and G. Tarjus, Eur. Phys. J. B **54**, 355 (2006).
[6] F. J. Pérez-Reche, M. L. Rosinberg, and G. Tarjus, Phys. Rev. B **77**, 064422 (2008).
[7] As a consequence of the no-passing rule [3], there cannot be metastable states outside the saturation hysteresis loop when using the standard ($\epsilon=0$) dynamics.
[8] B. Tadić, Phys. Rev. Lett. **77**, 3843 (1996).
[9] G.-P. Zheng and M. Li, Phys. Rev. B **66**, 054406 (2002).
[10] R. A. White and K. A. Dahmen, Phys. Rev. Lett. **91**, 085702 (2003).
[11] F. J. Pérez-Reche, B. Tadić, L. Mañosa, A. Planes, and E. Vives, Phys. Rev. Lett. **93**, 195701 (2004).
[12] F. Colaiori, G. Durin, and S. Zapperi, Phys. Rev. Lett. **97**, 257203 (2006).
[13] For a review, see B. K. Chakrabarti and M. Acharyya, Rev. Mod. Phys. **71**, 847 (1999).

[14] Since it is always the spin with the largest local field which triggers an avalanche, one can still use a "sorted-list" algorithm to speed up the computation, as proposed in M. C. Kuntz, O. Perković, K. A. Dahmen, B. W. Roberts, and J. P. Sethna, Comput. Sci. Eng. **1**, 73 (1999).

[15] M. Paczuski, S. Boettcher, and M. Baiesi, Phys. Rev. Lett. **95**, 181102 (2005).

[16] For $\sigma=1.5$, there is a spanning avalanche in the system and the value of H_{coer} computed in a small system may significantly differ from the actual value in the thermodynamic limit. However, for $L=24$, the shift in coercivity due to the change in ϵ is much larger than the error due to finite-size effects.

[17] O. Perković, K. A. Dahmen, and J. P. Sethna, Phys. Rev. B **59**, 6106 (1999).

[18] F. J. Pérez-Reche and E. Vives, Phys. Rev. B **67**, 134421 (2003).

[19] F. J. Pérez-Reche and E. Vives, Phys. Rev. B **70**, 214422 (2004).

[20] Only for $\epsilon=0.0005$, the curve corresponding to the smaller size $L=12$ could not be included in the collapse.

[21] Note that there are typically none or very few spanning avalanches along a half loop. Therefore, in order to reach good statistics for N_1 and N_2, it is not sufficient to analyze a few realizations of very large size.